Available online at www.sciencedirect.com

ScienceDirect

Procedia Engineering 101 (2015) 476 – 484

Procedia Engineering

www.elsevier.com/locate/procedia

3rd International Conference on Material and Component Performance under Variable Amplitude Loading, VAL2015

Three HCF models for strain fatigue life of welded pipes in austenitic stainless steel

Thomas Svensson[a,*], Dave Hannes[b], Pär Johannesson[c], Magnus Dahlberg[b], Andreas Anderson[c]

[a]TS Ingenjörsstatistik, Boviksvägen 21, 504 93 Borås, Sweden
[b]Inspecta Technology AB, Lindhagensterrassen 1, 104 25 Stockholm, Sweden
[c]SP Technical Research Institute of Sweden, 501 15 Borås, Sweden

Abstract

Fatigue bending tests have been performed on welded pipes made from an austenitic stainless steel. Four types of loading were used: 1) constant amplitude, 2) a load expected at pressure vessel environment, 3) a Gaussian load, and 4) a specially constructed two-level block load. The twenty-eight test results are evaluated using three different models: 1) the classical Basquin equation neglecting the fatigue limit, 2) the ASME model with a fatigue limit, and 3) a model with continuously decreasing fatigue limit. No significant differences between the three models were found. Predictions based on constant amplitude results appear to be non-conservative.

Peer-review under responsibility of the Czech Society for Mechanics

Keywords: austenitic stainless steel; welded pipe; experimental strain analysis; spectrum loading; high-cycle fatigue.

Nomenclature

a	factor in MD model
A	factor in ASME model
b	exponent or slope in MD model

* Corresponding author. Tel.: +46 705 409 771.
E-mail address: thomas.svensson@sinnesro.org

Peer-review under responsibility of the Czech Society for Mechanics
doi:10.1016/j.proeng.2015.02.057

B	exponent or slope in ASME model
C	asymptotic fatigue limit in ASME model
D	fatigue damage
i	dummy index
N	total number of cycles or predicted fatigue life
N_f	total number of cycles till failure
α	factor in ME model (Basquin)
β	exponent or slope in ME model (Basquin)
ε_a	strain amplitude
ε_{limit}	initial fatigue limit in MD model
$\hat{\sigma}$	estimated standard deviation of the errors

1. Introduction

Fatigue experiments on austenitic stainless steel are typically performed on small, smooth test specimens in air, whereas little experimental data is available for austenitic stainless steel components. The limited amount of component data available is almost exclusively dealing with constant amplitude testing for low-cycle fatigue (LCF). Extremely little experimental studies were performed on austenitic stainless steel components in the high-cycle fatigue (HCF) regime with variable amplitude loading. Such testing conditions correspond to more realistic loading scenarios of real-life components.

Austenitic stainless steels are challenging materials due to the non-linear material behaviour even for small amplitudes in a spectrum. Relative important inelastic deformations are observed when subjected to loads in the vicinity of the constant amplitude fatigue limit [1]. At variable amplitude loading the material behaviour is history dependent. Austenitic stainless steels are also subject to secondary cyclic hardening.

These complex features make it very difficult to find proper equivalence relations from simple specimens to components and it can be more efficient to find empirical strength properties by performing tests on component level. Of course, generalization is lost and more experimental efforts are needed, but in many applications this may be necessary to obtain more precise predictions. This study aims at increasing the knowledge about how to evaluate such an empirical approach. The current study aims also at making up for the shortcoming of experimental data on realistic austenitic stainless steel components, with particular focus on HCF and variable amplitude loading.

Stainless steel components were tested using constant and three different variable amplitude signals. The study of the experimental results was based on the use of three HCF models, which differ in their way of dealing with the fatigue limit. The models were applied assuming the linear damage accumulation rule or Palmgren-Miner rule [2,3], in accordance with the ASME procedure. The different fatigue models were used to investigate their predictive capabilities using different fatigue loading types. The results in the current investigation were obtained with a limited number of test specimens and realistic testing conditions. A new fixture for performing the experiments was developed.

2. Specimens

Initially a total number of 30 test specimens were manufactured from 60 straight, seamless TP 304 LE stainless steel pipes (Sandvik 3R12). The average chemical composition of the studied material is given in Table 1. The average material properties at room temperature are summarized in Table 2. The stainless steel pipes were approximately 400 mm long with an internal diameter of 49.25 mm. At one extremity of each pipe the wall-thickness was reduced to 3 mm, introducing shoulders at approximately 100 mm from the edge. These machined pipes were then joined with a circumferential butt weld, see Figure 1. The welding process was in compliance with nuclear requirements. Radiographic examination of all welding joints was performed according to EN 1435 B. Two circumferential butt welds were found not to comply with acceptance levels, as lack of fusion and/or pores were detected. These two tests specimens were removed from the current study, leaving a total number of 28 piping components for fatigue testing.

Table 1. Average chemical composition [wt%].

C	Si	Mn	P	S	Cr	Ni	Mo
0.011	0.38	1.14	0.020	0.006	18.25	10.11	0.10
W	Co	Ti	Cu	Nb	Ta	B	N
0.01	0.024	<0.005	0.048	<0.01	<0.005	<0.0004	0.057

Table 2. Average material properties at room temperature.

Yield strength [MPa]	Tensile strength [MPa]	Elongation [%]	Young's modulus [GPa]	Poisson's ratio [-]
281	616	52	200	0.3

Fig. 1. Finished test specimen after joining the separate machined pipes with a welding joint. The insert represents a close-up view of the circumferential butt weld, in as-welded condition.

3. Test equipment and loading spectra

In order to choose a suitable test method the aim was to subject the specimen to a state where a large portion of the material volume experiences the same stress levels. This approach will ideally allow a crack to initiate from anywhere inside this relatively large sub-volume and is therefore statistically more conservative when comparing to a test performed with a conventional notched test specimen. In order to obtain this state, a test set-up originating from bending was considered to be the best selection. As the tests should be performed as fatigue tests at a relatively high frequency a conventional 4-point bending method was considered to be unsuitable. While trying to minimize and to some extent exclude difficulties as wear at connections, mechanical play and complex stress distributions a design utilizing a torque arm connected to the test specimen was chosen. The set-up is presented in Figure 2 when mounted into a conventional single axis servo-hydraulic test machine. The only mechanical joints are where the torque arm is connected to the machine's axis of load.

This design will however not result in an ideal bending as the resulting axial force will induce a membrane stress superimposed to the stress resulting from bending. This force could be reduced by choosing a longer torque arm on the expense of the need for increased actuator amplitude reducing the test frequency. The arm length was chosen to be as long as possible while still resulting in a reasonable test frequency for the actual machine. With the final design it was possible to maintain a test frequency above 10 Hz and at the same time keep the superimposed membrane stress less than 5% of the bending stress, which was considered negligible for our purposes.

The tests were performed by mounting the specimens in an initially zero load condition. While being internally pressurized, the specimens were then subjected to a displacement controlled motion (spectra) resulting in a strain in the specimen measured in the longitudinal direction 50 mm from the center of the weld with a conventional strain gauge. This strain was during the initial experiments found to be linearly related to the applied motion. The average proportionality factor of 25.3 mm/% did slightly decrease towards the end of some tests with high strain amplitudes due to the presence of some non-linearity. The evaluation is however based on the continuously measured strains. The tests were continued until a leak occurred or until the run-out limit at 5 million cycles.

Fig. 2. Experimental set-up for fatigue testing of the piping components.

Tests were performed with constant amplitude and three different variable amplitude signals. The variable amplitude signals were simulated from level crossing specifications [4] and with irregularity factor, i.e. number of zero up-crossings over number of local maxima, close to unity. Each simulation had the block length of about 400-500 cycles and was repeated until specimen failure. One spectrum was generated from user specified level crossings, here called VAP, one spectrum was a Gaussian random process, VAG, and a third spectrum was a two-level block load, specially designed for the discrimination between different fatigue models, VA2. The two first spectra, VAP and VAG were applied to 7 and 6 specimens respectively, the third, VA2 to 5 specimens and constant amplitude, CA, load to 10 specimens.

4. Models for variable amplitude fatigue strength

Three models are considered to describe the fatigue strength of a particular welded pipe. The external load input to the models is chosen to be the measured global strain and the fatigue strength described by the number of cycles to failure. For variable amplitude loads, see [5], cycles are defined by rain-flow counting and the damage is assumed to occur according to the Palmgren-Miner rule [2,3].

$$D = \sum_{i=1}^{N} \frac{1}{N(\varepsilon_{a,i})}, \tag{1}$$

where D is the damage measure that equals unity at the limit state, i.e. when the component is expected to fail. The sum includes all N strain cycles that cause damage, and $N(\varepsilon_a)$ is the expected life for constant amplitude loading at the level ε_a.

The difference between the three models is how the fatigue limit, i.e. the load level that must be exceeded to cause damage, is included. The *Miner elementary* (ME) model assumes Basquin equation with no influence of the fatigue limit and assigns damage to all cycles in the load sequence. The *ASME model* (ASME) [6,7] assumes that there exists a fatigue limit and that the damage is calculated using the effective amplitude. The *Miner with decreasing fatigue limit* (MD) assumes that a fatigue limit is governed by a constant stress intensity threshold and thereby decreases during the load sequence evaluation [8].

For the Miner elementary (ME), the expected fatigue life is modelled by the Basquin equation,

$$N = \alpha(\varepsilon_a)^{-\beta}, \tag{2}$$

which is applied for all counted strain cycles. For the ASME model (ASME), the expected fatigue life is modelled by the model used for the derivation of the design curve in the ASME Boiler and Pressure Vessel Code [9],

$$N = A(\varepsilon_a - C)^{-B}, \tag{3}$$

for strain cycles exceeding C, and infinite life otherwise. The parameter C thereby acts as an asymptotic fatigue limit. For the Miner with decreasing fatigue limit (MD), the expected fatigue life is modelled by the Basquin equation, see Eq. (2), for each cycle that exceeds the fatigue limit. The fatigue limit is assumed to be related to the stress intensity threshold of a growing crack. For variable amplitude loading this means that each single strain cycle that exceeds the fatigue limit corresponding to the present crack will cause growth and thereby decrease the actual fatigue limit. By assuming that the variable amplitude load is a stationary random process, this theory leads to a manageable model that only needs the Basquin parameters and the initial fatigue limit as input.

The study of variable amplitude loading is based on the definition of a variable amplitude scalar metric that is consistent with the selected fatigue model. The *strain beta norm* was introduced as,

$$\left\|\{\varepsilon\}\right\|_{\beta} = \left(\frac{1}{N_f} \sum_{i=1}^{N_f} (\varepsilon_{a,i})^{\beta} \right)^{1/\beta}, \tag{4}$$

where $\{\varepsilon\}$ is the load sequence used for the test and N_f is the total number of cycles to failure, see details in [10]. In case of the presence of a fatigue limit the sum just contains strain cycles that exceed the limit. This metric is then used in place of the constant strain amplitude in the fatigue models described above.

5. Experimental results

The obtained experimental results for the different loading spectra are presented in Figure 3.

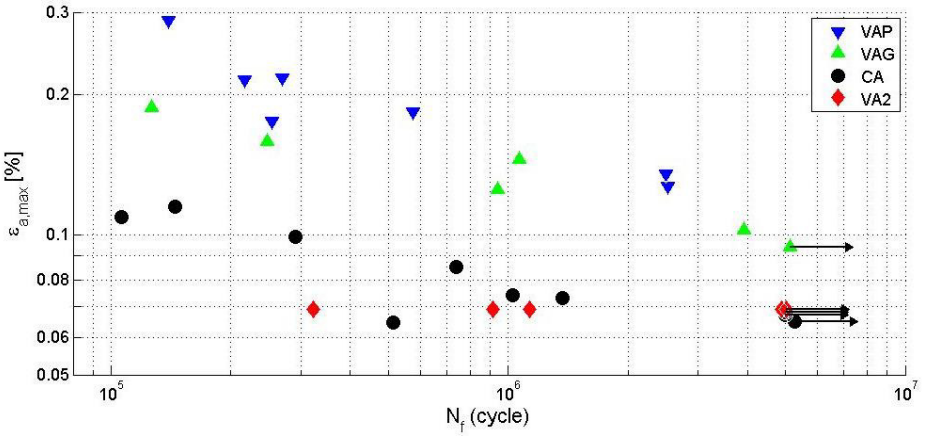

Fig. 3. Experimental data from the 28 fatigue tests. The maximum strain amplitude was used on the ordinate axis. The data points with a horizontal arrow represent run-outs.

5.1. Parameter estimation

For parameter estimation, the maximum-likelihood method was used, which is a probabilistic method. The logarithm of the observed life is assumed to follow a normal distribution with expected value according to the models, and disturbed by a random error for each individual test. By maximizing the likelihood, i.e. the probability for the actual observations, with respect to the model parameters, estimates both for the model parameters and the standard deviation of the errors are found, see [10] for more details on the methodology.

The data used for the first estimate are the thirteen tests performed with variable amplitude spectra, VAP and VAG. Separate estimates were initially done for each spectrum type, but since no significant difference was detected, they were judged to be similar within the model and an estimate using results from both types were used together. The possibility to this combination is a nice property of the fatigue norm approach used here, which is advantageous compared to the Gassner curve approach [11,12]. The estimated parameters are summarized in Table 3. In Figure 4, the three models are illustrated in the same diagram for comparison. The diagram is constructed in the following way: Gaussian reference spectra are constructed by scaling the spectrum strain levels used in the tests. Scale factors are used to cover a suitable range of predicted lives. For each such reference spectrum, fatigue life is predicted using the three models above with the estimated parameters. The result is plotted against the strain beta norm of each reference spectrum. In addition, lower 90% prediction limits representing 95% survival probability, are illustrated.

The parameter estimation using the constant amplitude tests was performed in a similar way, see also Table 3. The fatigue limit for the MD model was however estimated separately from failure/run-out results, and the Basquin parameters were then estimated based on results with strains exceeding the fatigue limit.

Table 3. Estimated model parameters and the estimated standard deviation of the errors, $\hat{\sigma}$.

Fatigue model	Data	Factor estimates		Exponent (slope) estimates		Limit [%] estimates		$\hat{\sigma}$
ME	VAP+VAG	α	1.06	β	4.6			0.42
	CA		0.49		5.66			0.75
ASME	VAP+VAG	A	128	B	2.01	C	0.058	0.36
	CA		10.4		4.28		0.00096	0.49
MD	VAP+VAG	a	3.51	b	4.45	ε_{limit}	0.076	0.42

	CA	1.99	0.066	0.26

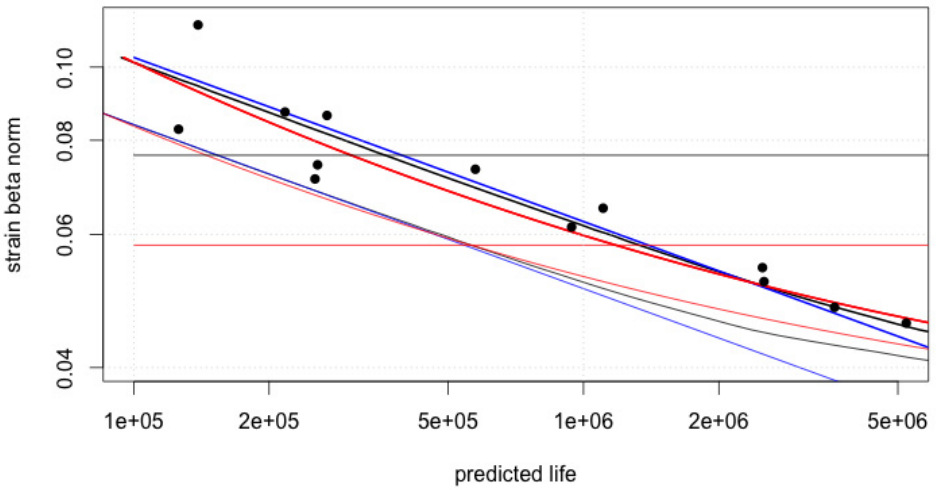

Fig. 4. Estimated fatigue models based on VAP + VAG data, represented as black dots. The strain beta norm was computed with β=4.6. The colour legend of the curves is: ME: blue, ASME: red and MD: black. The horizontal lines represent the estimated fatigue limits.

5.2. Prediction of special spectrum by both approaches

Based on the estimated results from the variable amplitude tests (VAP+VAG), a special spectrum was designed with the purpose of discriminating between the three models. Since the difference is related to the interpretation of the fatigue limit, it was found that a simple two-level spectrum should suffice, denoted VA2. The high amplitude was chosen to 0.069 % which is below the estimated fatigue limit in the MD case and thereby should give infinite life. The lower amplitude was chosen to 0.042 % which is below the fatigue limit estimate in the ASME case. Using the estimated models the following lives were predicted: 1.2 10^6, 2.2 10^6 and infinity, for the ME, the ASME and the MD model respectively.

The five experimental results using the VA2 spectrum are shown in Figures 1 and 5. The median of these results is 1.1 10^6. However, the scatter is considerable. In the Figure 5, the three models based on variable amplitude data are illustrated by solid lines, the models estimated from constant amplitude tests by dashed lines and the five VA2 test results as black dots. Denote that the rightmost dot represents a run-out.

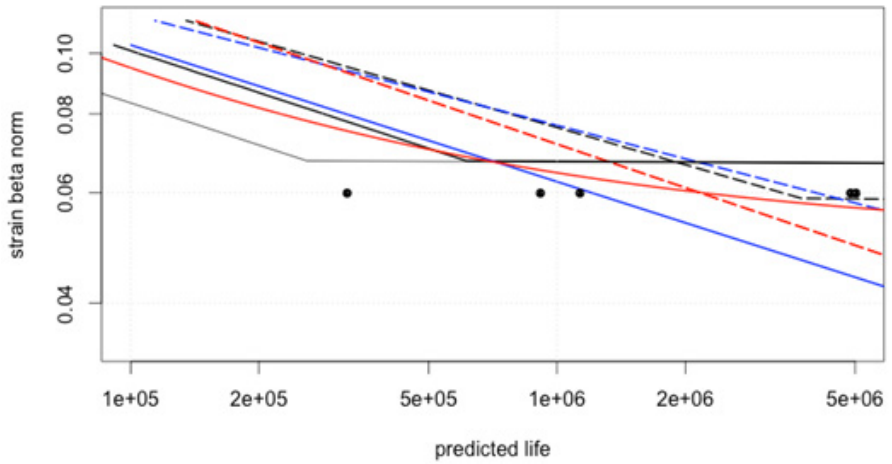

Fig. 5. Estimated fatigue models based on VAP+VAG data (solid lines) and CA data (dashed lines) with the VA2 data points represented as black dots. For the colour legend, see Figure 4. Diagram constructed using VA2 as reference spectrum.

6. Discussion and conclusions

The tests performed here were easily performed in an ordinary test machine at fully reversed load, thanks to the newly developed test fixture. By applying spectrum load and using a welded pipe with internal pressure, the test represents conditions close to real pressure vessel applications.

The fatigue results show a considerable scatter, about 40-50% in life, and it is thereby difficult to judge about the differences between the investigated models for fatigue life. Referring to Figure 4, one can observe that the median estimated curves are quite similar but that the lower prediction limits differ a lot for long lives. The two models that include the fatigue limit give narrower prediction band than Miner elementary, which is important for deciding safety factors in design. This result, however, is obtained by using variable amplitude reference tests. If we compare to the corresponding curves based on constant amplitude, illustrated in Figure 5, they predict considerably longer lives and appear to be non-conservative.

The trial to discriminate between the three models unfortunately failed. The reasons are twofold, firstly the scatter at this low strain level is larger than in the reference tests and secondly the test spectrum had to be chosen to obtain results within reasonable testing time. If it had been possible to use a resonance machine instead of a servo-hydraulic, then the maximum life could have been extended and a more discriminating spectrum could have been used. It would therefore be desirable to perform tests in a high frequency resonance machine to make a more thorough study of the behaviour around the fatigue limit.

In many applications this low strain domain is of utmost importance, since designs often aim at lives longer than a million cycles. One can conclude that constant amplitude tests tend to give non-conservative estimates when using the Palmgren-Miner cumulative damage rule. The scatter, typical for fatigue, makes it difficult to discriminate between the models, and thus find the best model for life prediction.

Acknowledgements

The authors gratefully acknowledge the financial support from the Swedish Radiation Safety Authority, SP Technical Research Institute of Sweden and Ringhals AB. The austenitic stainless steel seamless pipes used during manufacturing of the investigated test specimens were kindly provided by Sandvik AB.

References

[1] J. Colin, A. Fatemi, Variable amplitude cyclic deformation and fatigue behaviour of stainless steel 304L including step, periodic, and random loadings, Fat. Fract. Eng. Mat. Struct., 33 (2010), 205 – 220.
[2] A. Palmgren, Die Lebensdauer von Kullagern, Zeitschrift des Vereins Deutscher Ingenieure, 1924, 339–341, (In German).
[3] M.A. Miner, Cumulative damage in fatigue, J.Appl. Mech., 12 (1945), 159–164.
[4] T. Svensson, Fatigue testing with a discrete-time stochastic process, Fat. Fract. Eng. Mat. Struct., 17(1994), 727 – 736.
[5] P. Johannesson, M. Speckert (Eds.), Guide to Load Analysis for Durability in Vehicle Engineering, Wiley: Chichester, 2013.
[6] B. F. Langer, Design of Pressure Vessels for Low-Cycle Fatigue, ASME J. Basic Eng., 84 (1962), 389– 402.
[7] O. K. Chopra, W. J. Schack, Effect of LWR Coolant Environments on the Fatigue Life of Reactor Materials, NUREG/CR-6909, 2007.
[8] T. Svensson, Cumulative fatigue damage taking the threshold into account, Fat. Fract. Eng. Mat. Struct., 25 (2002), 871– 876.
[9] ASME Boiler and Pressure Vessel Code – Division III, Rules for Construction of Nuclear Facility Components, 2013.
[10] P. Johannesson, T. Svensson, J. de Maré, Fatigue life prediction based on variable amplitude tests - methodology, Int. J. Fatigue, 27 (2005), 954–965.
[11] E. Gassner, Betriebsfestigkeit, eine Bemessungsgrundlage für Konstruktionsteile mit statistisch wechselnden Betriebsbeanspruchungen, Konstruktion, 6 (1954), 97–104, (In German)
[12] P. Johannesson, B. Johannesson, T. Svensson, M. Karlsson, Statistical analysis of constant and different variable amplitude spectra. Proc. Fatigue 2007, Cambridge, UK, 26-28 March, 2007.